Mechanical Systems and Signal Processing 85 (2017) 993–1004

Contents lists available at ScienceDirect

Mechanical Systems and Signal Processing

journal homepage: www.elsevier.com/locate/ymssp

Source distance determination based on the spherical harmonics

Adam Koutny[a,*], Ondrej Jiricek[a], Jean-Hugh Thomas[b], Marek Brothanek[a]

[a] Czech Technical University in Prague, Technicka 2, 166 27 Prague, Czech Republic
[b] Laboratoire d'Acoustique de l'Université du Maine (LAUM-UMR CNRS 6613) and École Nationale Supérieure d'Ingénieurs du Mans, rue Aristote, 72085 Le Mans Cedex 09, France

ARTICLE INFO

Keywords:
Microphone array
Spherical array
Spherical harmonics
Near-field acoustical holography

ABSTRACT

This paper deals with the processing of signals measured by a spherical microphone array, focusing on the utilization of near-field information of such an array. The processing, based on the spherical harmonics decomposition, is performed in order to investigate the radial-dependent spherical functions and extract their argument – distance to the source. Using the low-frequency approximation of these functions, the source distance is explicitly expressed. The source distance is also determined from the original equation (using no approximation) by comparing both sides of this equation. The applicability of both methods is first presented in the noise-less data simulation, then validated with data contaminated by the additive white noise of different signal-to-noise ratios. Finally, both methods are tested for real data measured by a rigid spherical microphone array of radius 0.15 m, consisting of 36 microphones for a point source represented by a small speaker. The possibility of determination of the source distance using low-order spherical harmonics is shown.

1. Introduction

The genuine three-dimensional symmetry of the spherical microphone array makes such an array a very strong and powerful tool capable of operating in complex reverberant fields enabling a description of a field radiated by a vibrating structure. Recently, the spherical array itself as well as the corresponding signal processing has been the subject of ongoing research. It has been advantageously utilized in sound source localization and sound field reconstruction techniques such as beamforming and near-field acoustical holography, respectively [1–4]. The analysis based on the spherical harmonics decomposition and the design of such an array is theoretically presented in a recent papers [5,6] and subsequent references. An exhaustive description of the sound field expansion in terms of the spherical harmonics can be found in [7]. Previous studies dealing with sound field analysis by a spherical array assumed the sources to be placed in the far-field of an array [8,5,9]. The capabilities of an array in its near-field have been presented in very recent papers [10,11] together with the definition of this close region, or in compact form in [12]. The capability of capturing the spherical wavefront radiated by a source (in the near-field of an array) provides additional information that can be utilized in processing.

The main objective of beamforming-based methods is the determination of the direction(s) of the arrival of sound wave(s) radiated by a far-field source(s) [13]. Such an analysis usually provides a map of sources surrounding the measurement array. On the contrary, holography-based techniques exploit the near-field information in order to increase the spatial resolution of reconstruction. Considering the interior problems, in which all the sources are located outside a certain sphere (the measurement sphere), the theory of spherical near-field acoustical holography, summarized in [7], makes the reconstruction of the surrounding sound field

* Corresponding author.
E-mail address: koutnada@fel.cvut.cz (A. Koutny).

http://dx.doi.org/10.1016/j.ymssp.2016.09.015
Received 29 July 2014; Received in revised form 17 June 2016; Accepted 10 September 2016

possible up to the distance of the nearest source. The *a priori* knowledge of the source position (mainly the distance from an array – in the case of a spherical array) may not be easy to achieve. For example, while attempting to reconstruct the sound field generated by a source moving in the near-field of an array [14] as close to the source as possible, it could be impractical to measure the source distance "manually". Therefore, this paper deals with the utilization of the near-field information in order to determine this distance numerically from the measured data. The idea of determination of the source distance based on the measured data appeared in [15].

The method described in this article assumes the characteristic of the sources to be similar to the point source (such as sources of radiating sections that are relatively small in relation to their operating wavelengths). The aim of this method is to determine the distances to such sources based exclusively on the measurement data. To emphasize this assumption, we will use the notation *origin of a spherical wave* instead of *the source* in the following description. It is also assumed that, in certain applications, such sources could be separated in the spatial and/or time domain by common separation methods (e.g. blind source separation, etc.). Moreover, the determined distance could be further utilized in the source extraction methods, such as the Point Source Separation (PSS) method, in which multiple incoherent point sources in a free field are assumed [16]. Once the point source locations are determined, the interfering signals could be separated by PSS. Note that in connection with a spherical array consisting usually of quite a large number of microphones (with respect to common separation/extraction method assumptions; e.g. 4 in mentioned reference), the PSS method could decompose particularly complex sound fields. An example of a real application could be the determination of the distance to the speaker's mouth, in which a manual measurement is not convenient, especially when the speaker's movement is expected.

In Section 2, processing based on spherical harmonics, which is used for the determination of the distance to the origin of a spherical wave, is briefly reviewed. In Section 3, the basic design parameters of the spherical array focusing on its near-field are discussed. Then in Section 4, the distance to the origin of a spherical wave based on the Fourier coefficients is validated using the model data set. The validation using the data measured by a rigid spherical microphone array consisting of 36 microphones is performed in Section 5 followed by discussion of the uncertainty and the Monte Carlo simulation in Section 6. Finally, the results are summarized in Section 7.

2. Spherical array signal processing

In this section, processing based on the spherical harmonics decomposition is briefly reviewed and subsequently focused on the performance in the near-field of an array.

2.1. Spherical Harmonics-based Signal Processing

Spherical harmonics decomposition represents an integral transform, in which the basis functions are represented by harmonic functions defined on the spherical surface (the spherical Fourier transform). These harmonic functions satisfy the spherical wave equation for angular variables (elevation and azimuth). Thorough description of these functions is given in [7].

Consider the acoustic pressure p to be measured on a sphere of radius r=a. Employing the standard spherical coordinate system (r, θ, ϕ) [7], the spectrum (marked by variable ω) of measured pressure $p(a, \theta, \phi, \omega)$ can be decomposed as

$$p\left(a, \theta, \phi, \omega\right) = \sum_{n=0}^{\infty} \sum_{m=-n}^{n} P_{mn}\left(a, \omega\right) Y_n^m\left(\theta, \phi\right), \tag{1}$$

where $Y_n^m(\theta, \phi)$ are the spherical harmonics composing an orthonormal system of functions defined using the associated Legendre functions $P_n^m(\cos\theta)$ as

$$Y_n^m\left(\theta, \phi\right) = \sqrt{\frac{(2n+1)}{4\pi}\frac{(n-m)!}{(n+m)!}} P_n^m\left(\cos\theta\right) \mathrm{e}^{\mathrm{i}m\phi}, \tag{2}$$

where j stands for the imaginary unit and integer numbers n and m represent the orders and all corresponding degrees ($m \in [-n, n]$), respectively. In Eq. (1), $P_{mn}(a, \omega)$ are the Fourier coefficients given by the forward spherical Fourier transform

$$P_{mn}\left(a, \omega\right) = \int\int p\left(a, \theta, \phi, \omega\right) Y_n^{m*}\left(\theta, \phi\right) \sin\theta \mathrm{d}\theta \mathrm{d}\phi, \tag{3}$$

where the integration is performed over a sphere. The coefficients P_{mn} will be used in Section 4 for the determination of the distance to the origin of a spherical wave. The asterisk stands for the complex conjugation. Since the spherical harmonics represent the modes of a sphere, the processing is sometimes referred to as phase-mode processing in connection with beamforming techniques [8]. The radial dependence of these basis functions focusing on the region close to an array is discussed in the next section.

2.2. Near-field spherical microphone array

The transition between the near and the far field of an array is usually related to the approximation error of spherical wavefront in relation to the plane wave. Therefore, in the case of the capability of an array to capture the spherical wavefront, such information could be advantageously utilized for not only distance determination, but also for better spatial separation of multiple sources [11]. As expected, the array near field capabilities depend on its design as well as the processing frequency. The radial processing focusing

on this close region of an array is reviewed in this section. In designing the spherical microphone array, the critical parameters influencing its spatial resolution are the total number of the microphones spatially sampling the surrounding sound field, as well as their distribution around the sphere surface – for detailed discussion on this topic see [6]. These parameters restrict the maximum order of spherical harmonics $N = \max(n)$ that could be used in processing without any aliasing effect (considering the surrounding sound field to be harmonic-order limited, $P_{mn} = 0: \forall\, n > N$). This restriction limits the infinite summation in Eq. (1) up to the order n=N and discretizes the spherical Fourier transformation in Eq. (3). The error caused by this limitation is usually termed the *base system error* and diminishes to zero as N increases to infinity [3].

To evaluate the near-field information, the plane wave (generated by a source at infinity – in the far field) and the spherical wave (generated by a source in the near field of an array) impinging the measurement sphere are to be studied separately. The corresponding Fourier coefficients can be expressed as [11]

$$P_{mn}\left(a,\,\omega\right) = \begin{cases} b_n(k,\,r)\,Y_n^{m*}(\theta_0,\,\phi_0), & \text{for plane wave,} \\ b_n^s(k,\,r,\,r_s)\,Y_n^{m*}(\theta_s,\,\phi_s), & \text{for spherical wave,} \end{cases} \tag{4}$$

where $(\theta_0,\,\phi_0)$ represents the direction of propagation of the plane wave, $(r_s,\,\theta_s,\,\phi_s)$ represents the location of point source and k is the wavenumber. The so-called *far-field mode-strength function* $b_n(k,\,r)$ derived for an open and rigid sphere considering the plane wave impinging the sphere can be expressed as

$$b_n(kr) = 4\pi \mathrm{i}^n \begin{cases} j_n(kr) & \text{for open sphere,} \\ j_n(kr) - \dfrac{j_n'(ka)}{h_n'(ka)} h_n(kr) & \text{for rigid sphere,} \end{cases} \tag{5}$$

where j_n represents the spherical Bessel function of the first kind of order n, and h_n represents the spherical Hankel function of the first kind of order n. The prime stands for the derivative with respect to the argument. While the rigid sphere influences the surrounding sound field by its acoustically hard surface (zero surface velocity), the open sphere is considered acoustically transparent and does not influence the sound field.

On the contrary, assuming the point source located in the near-field of an array (a spherical wave impinging the sphere), the analogous *near-field mode-strength function* is

$$b_n^s(k,\,r,\,r_s) = \mathrm{i}^{-(n-1)} k b_n(kr) h_n(kr_s). \tag{6}$$

By exploring Eq. (6) (using $b_n(kr)$ for the open and rigid sphere defined in Eq. (5)) it is clear that the spherical wave behavior is embodied by the function $h_n(kr_s)$. By graphical comparison of both plane and spherical mode-strength functions (see Fig. 3 in [11]), the near field criterion can be expressed as

$$r_{\mathrm{NF}} \approx \frac{N}{k}. \tag{7}$$

In this region, the possibility of capturing spherical wavefront by an array can be assumed. Note the dependency on array design hidden in the maximal order N and dependency on frequency, as mentioned earlier. Determination of the distance $r_s \le r_{\mathrm{NF}}$ is the subject of the next section.

3. Determination of the distance to the origin of a spherical wave

In this section, the determination of the distance r_s based on the spherical Fourier coefficients of the measured pressure is described. The motivation of such approach is gained by the possibility of distance determination in situations, in which the direct measurement by mechanical or optical meter is impractical and/or complicated. Starting with the simple determination of distance of the static point source, this approach could find its usability in case of the point-like source moving in the near field of an array. Moreover, the generalization of this method for more complicated and/or multiple sources including the source separation processing techniques is the subject of further research.

The *overall spherical wave mode-strengths* can be calculated for all possible spherical modes (the orders n of spherical harmonics) from the Fourier coefficients (Eq. (4)) of all respective degrees $m \in [-n,\,n]$ as

$$\sum_{m=-n}^{n} |P_{mn}|^2 = \frac{(2n+1)}{4\pi} |b_n^s(k,\,r,\,r_s)|^2, \tag{8}$$

utilizing the equality

$$\sum_{m=-n}^{n} |Y_n^m(\theta,\,\phi)|^2 = \frac{(2n+1)}{4\pi}.$$

Eq. (8) represents the overall strength of the corresponding spherical mode of order n. The determination is based on the division of two adjacent mode-strengths

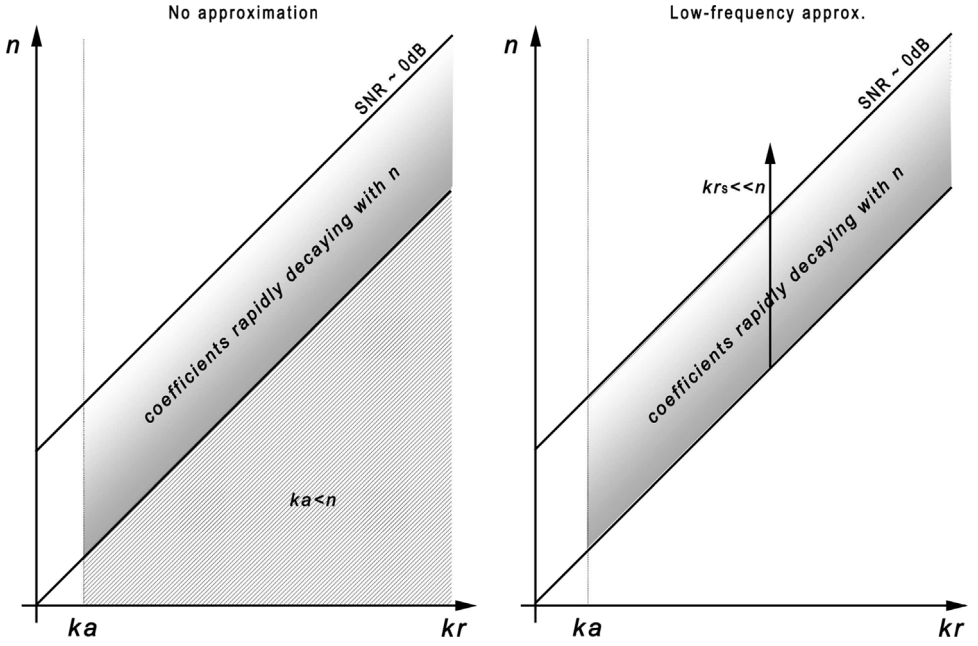

Fig. 1. Regions of applicability of both methods. *Left*: no-approximation method, the region of applicability is depicted by hatched together with shaded area. *Right*: with low-frequency approximation, the region of applicability is depicted by shaded area.

$$\frac{\sum_{m=-n}^{n}|P_{m,n+1}|^2}{\sum_{m=-n}^{n}|P_{mn}|^2}=\frac{(2n+3)|b_{n+1}^{s}(k,r,r_s)|^2}{(2n+1)|b_n^{s}(k,r,r_s)|^2}=\frac{(2n+3)|b_{n+1}(kr)h_{n+1}(kr_s)|^2}{(2n+1)|b_n(kr)h_n(kr_s)|^2}. \tag{9}$$

In the following sections, the derivation is first presented in the case without any approximation of the radial functions, and then with the approximation valid for low frequency assumption.

3.1. No approximation

By dividing two adjacent mode strengths (see Eq. (9)) and expressing for the distance-dependent functions, one can obtain the equation

$$\frac{|h_{n+1}(kr_s)|^2}{|h_n(kr_s)|^2}=\frac{\left(2n+1\right)\left|b_n(ka)\right|^2\sum_{m=-(n+1)}^{n+1}\left|P_{m,n+1}\right|^2}{(2n+3)|b_{n+1}(ka)|^2\sum_{m=-n}^{n}|P_{m,n}|^2}. \tag{10}$$

While the left-hand side of Eq. (10) is exponentially decaying with respect to the argument, the right hand side is a constant for the given configuration (a, n, k). Therefore, finding the equality of both sides leads to the determination of the distance to the origin of a spherical wave. Although it is possible to use an arbitrary value of n for the determination, the maximum order is always subject to the signal-to-noise ratio. The nature of the Fourier coefficients has already been discussed in [3], in which the rapid decay of the coefficients while $n > ka$ has been demonstrated. This behavior is also obvious in our model validation. In the left part of Fig. 1, the area of applicability of this method is shown (hatched together with shaded) depending on the order n of spherical harmonics and kr. Note that the above-mentioned condition for the coefficients is not as strict, and is represented by the upper diagonal line (SNR $\approx$ 0 dB). Those coefficients that are above the noise level are still usable for the determination. Therefore, the applicability of this method is limited for higher orders, whose coefficients are significantly influenced by the noise.

3.2. Low-frequency approximation

Our earlier results of the distance determination using the approximation-based method have been presented in [17]. Considering $kr_s \ll n$, it is possible to approximate spherical radial functions (j_n and h_n) and extract the distance r_s. Again, by dividing two adjacent mode strengths (see Eq. (9)) and using the approximations [7]

$$\frac{|h_{n+1}(kr_s)|}{|h_n(kr_s)|}\approx\frac{2n+1}{kr_s} \tag{11}$$

and

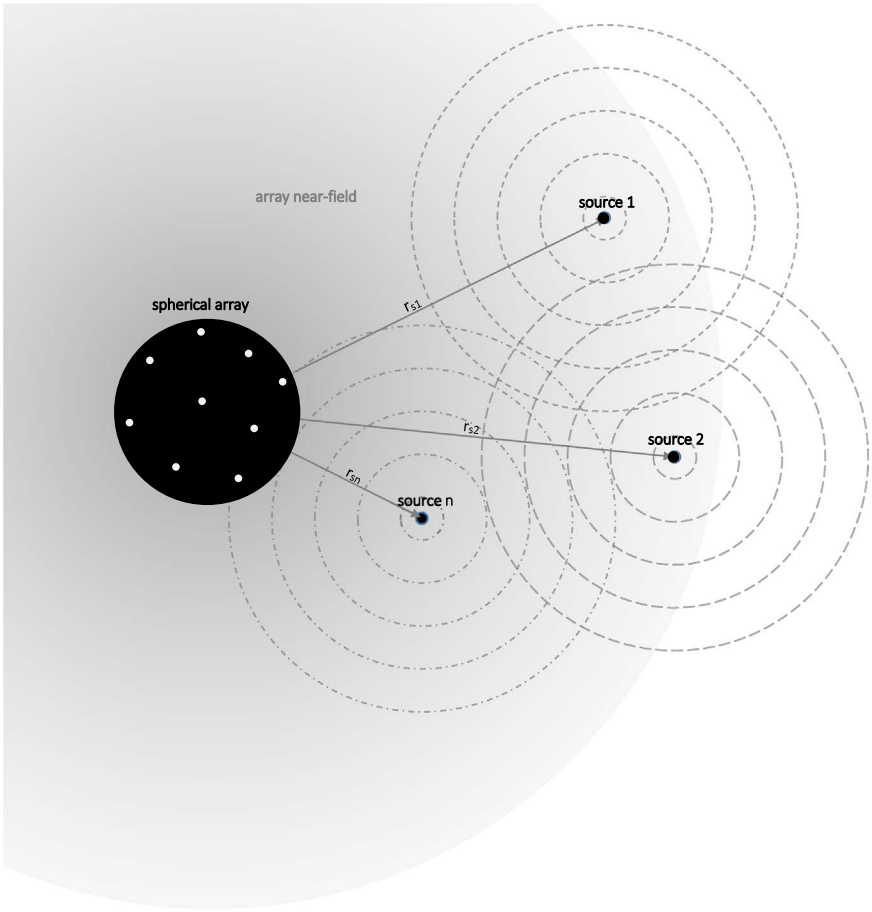

Fig. 2. A scheme of typical experiment.

$$\frac{|b_{n+1}(ka)|}{|b_n(ka)|} \approx \frac{ka(n+1)}{(2n+1)(n+2)}, \tag{12}$$

the latter being valid for the rigid sphere (not for the open sphere), the distance to the origin of a spherical wave can be extracted and expressed as

$$r_s = a\sqrt{\frac{(2n+3)(n+1)^2\sum_{m=-n}^{n}|P_{m,n}|^2}{\left(2n+1\right)(n+2)^2\sum_{m=-(n+1)}^{n+1}\left|P_{m,n+1}\right|^2}}. \tag{13}$$

In similar way, the area of applicability is shown in the right part of Fig. 1. In this case, the consideration used for approximation restricts the usable coefficients to only those satisfying both conditions.

4. Model validation

In this section, both methods are validated using the model data represented by a point source located at distance $r_s = 0.3$ m from the origin (center of the sphere) for three different signal-to-noise ratios (SNR, modeled using the MATLAB function *awgn* as the ratio of signal power to noise power). For the purposes of this article, the array performance is evaluated according to the maximum order N while the aliasing effect is not considered – the model sphere of radius a=0.15 m is sampled in many more points than would be adequate for the given order. The Fourier coefficients are calculated according to Eq. (3) implemented by the Singular Value Decomposition (SVD). This approach is described in [3]. The determination for the order n, labeled in following pictures and tables, is performed using this order and the $(n+1)$ order (division of two adjacent mode strengths). A scheme of a typical experiment is depicted in Fig. 2.

4.1. Noise-less data

Firstly, the ideal situation with a model point source with $kr_s = 2.77$ (f=500 Hz) with no added noise is exemplarily shown in

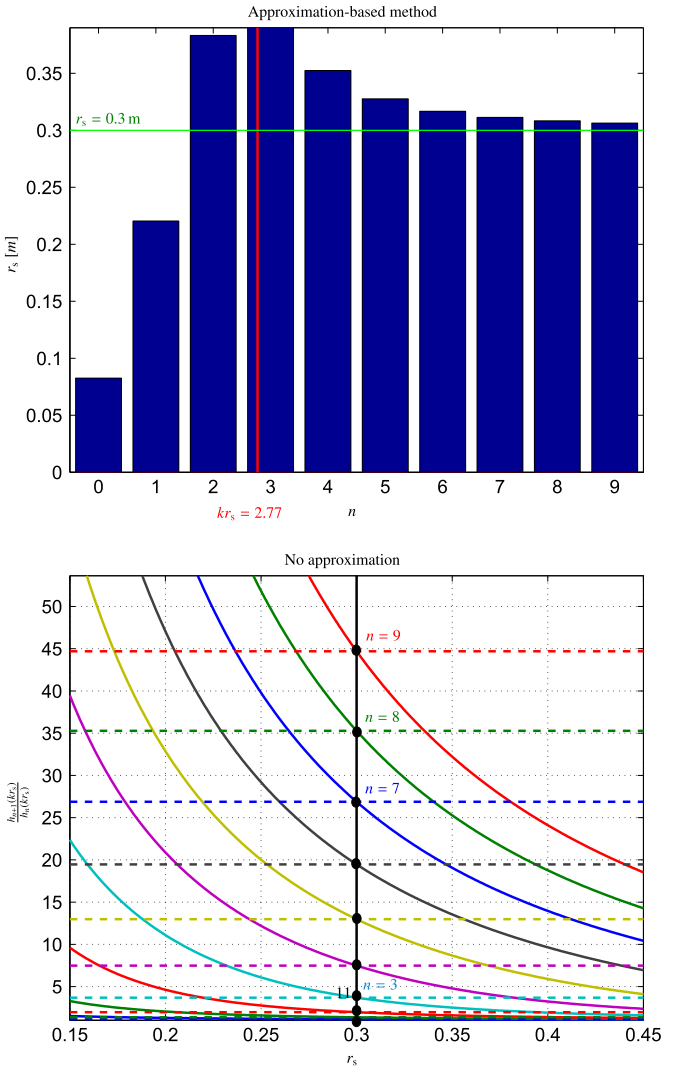

Fig. 3. Noise-less data model simulation. *Top*: approximation-based method. *Bottom*: no-approximation method. The determination for the order n, labeled in the pictures, is performed using this order and the $(n + 1)$ order (division of two adjacent mode strengths). (For interpretation of the references to color in this figure caption, the reader is referred to the web version of this paper.)

Table 1
Noise-less data model simulation. Determined values of r_s (m). True value is $r_s = 0.3$ m and $kr_s = 2.77$.

Method	Order									
	0	1	2	3	4	5	6	7	8	9
Approx. r_s (m)	0.08	0.22	0.38	0.39	0.35	0.33	0.32	0.31	0.31	0.31
No approx. r_s (m)	0.30	0.30	0.30	0.30	0.30	0.30	0.30	0.30	0.30	0.30

Fig. 3. The results of the approximation-based method are presented in the top part of this figure while the results of the no-approximation method are presented in the bottom part. The determination is performed up to n=10 to show the convergent behavior (to the true source distance shown by the *green* horizontal line) of the approximation-based method; however, according to the above discussed validity of this method, the higher orders will not be useful in the case of noisy data. The *red* vertical line representing the actual value of kr_s is shown to evaluate the fulfillment of the approximation condition $kr_s \ll n$. In the bottom picture, the left-hand side of Eq. (10) is depicted for the given orders by solid curves, while the constant values of the right hand side are depicted by dashed lines. The mutual intersections are highlighted by the dots and actual distance is represented by the *black* vertical line. Of course, the same as before holds for higher orders, however, the determination is not limited at the lower orders. The determined distances are presented in Table 1 as well – the values in gray-marked cells do not satisfy the approximation condition

and cannot be considered as usable results in general. Such an array capable of processing the data up to the 10th order would be, according to Eq. (7), able to utilize the near-field information up to the distance r_{NF} = 1 m at f=500 Hz. Nonetheless, it should be noted that the required number of microphones is related to the maximum order N of the spherical harmonics. For example, considering *nearly uniform sampling scheme* discussed in [6] the required number of microphones would be at best $(N+1)^2$, but in practice larger.

4.2. Noisy data

The second model example shows the distance determination while the noise-less data were contaminated by the additive white noise of SNR=15, 10 and 5 dB. As has been already discussed, the noise mainly influences the higher orders, whose coefficients are comparable to the noise level. This finding applies for both methods, as clearly seen in Fig. 4. In this case, the determination becomes significantly erroneous for orders higher than 4. The bottom part of this figure shows the possibility of distance determination using Eq. (10) – the behavior of determination using lower orders will become clear from the following table. The determined distances can be seen in Table 2 for three different SNR. These values represent the average values of five realizations. The gray-marked values do not satisfy the approximation condition. The graphic representation of these values can also be seen in Fig. 5.

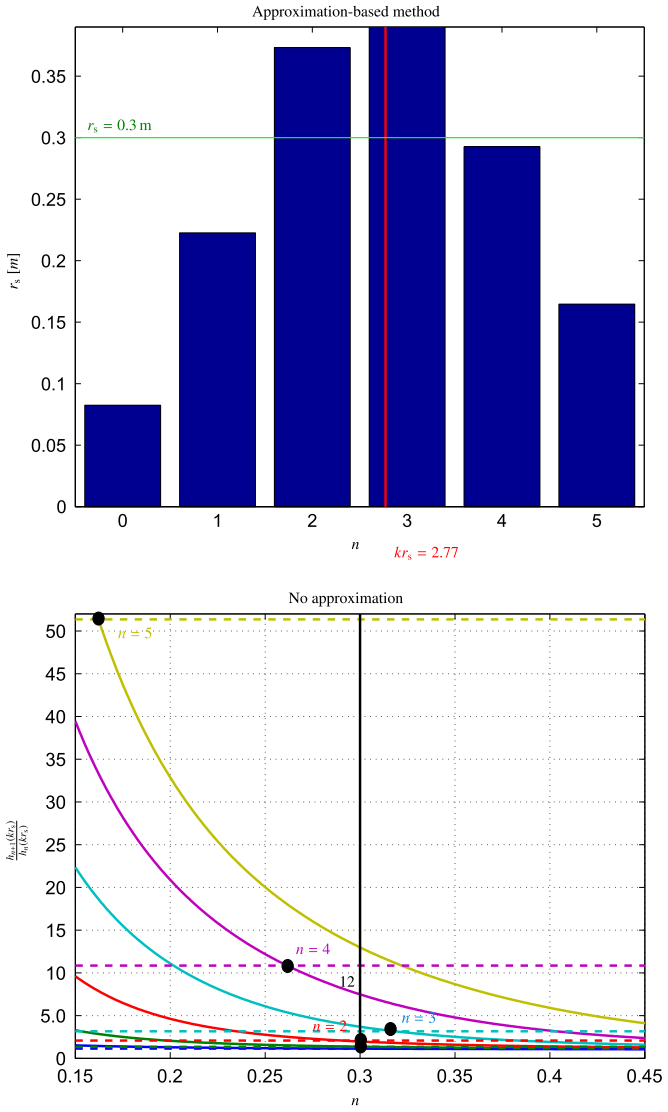

Fig. 4. Noisy data model simulation – SNR=15 dB. Results of one realization. *Top*: approximation-based method. *Bottom*: no-approximation method. The determination for the order n, labeled in the pictures, is performed using this order and the $(n+1)$ order (division of two adjacent mode strengths).

Table 2
Noisy data model simulation. The average values of five realizations of the determination of r_s (m). The true value is $r_s = 0.3$ m and $kr_s = 2.77$.

Method	SNR=15 dB					
	Order					
	0	1	2	3	4	5
Approx. r_s (m)	0.08	0.22	0.38	0.38	0.30	0.19
No appr. r_s (m)	0.30	0.30	0.30	0.29	0.27	0.19
	SNR=10 dB					
Approx. r_s (m)	0.08	0.22	0.37	0.40	0.23	0.16
No appr. r_s (m)	0.33	0.30	0.29	0.31	0.21	0.17
	SNR=5 dB					
Approx. r_s (m)	0.08	0.22	0.35	0.31	0.21	0.15
No appr. r_s (m)	0.36	0.29	0.28	0.25	0.20	0.16

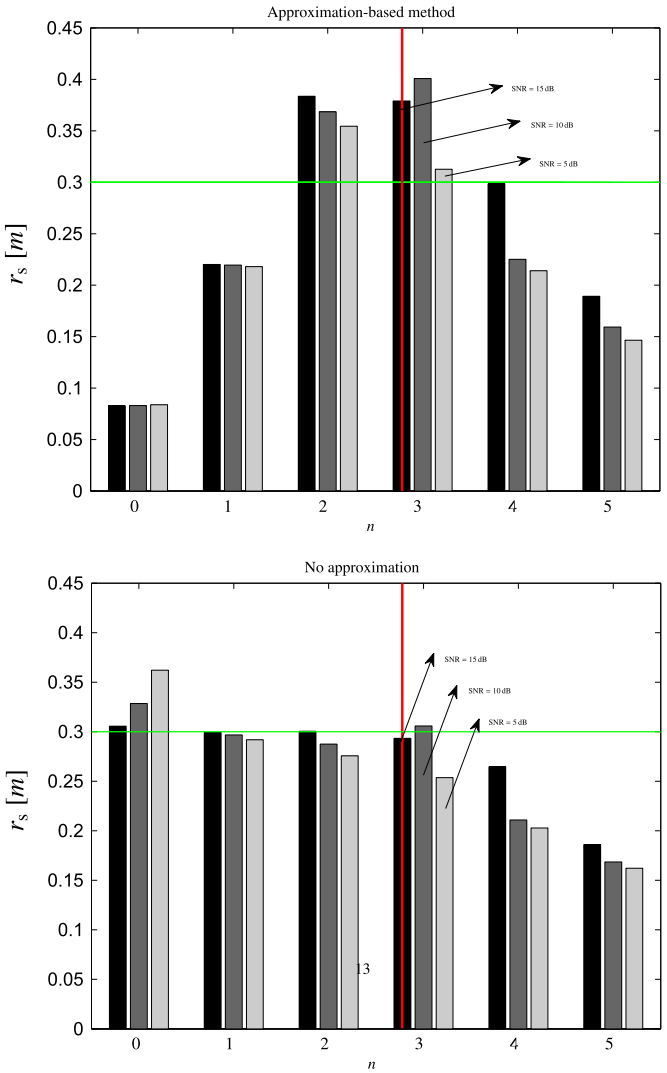

Fig. 5. Noisy data model simulation. Average values of five realizations of the determination of r_s (m). *Top*: approximation-based method. *Bottom*: no-approximation method. The determination for the order n, labeled in the pictures, is performed using this order and the $(n + 1)$ order (division of two adjacent mode strengths).

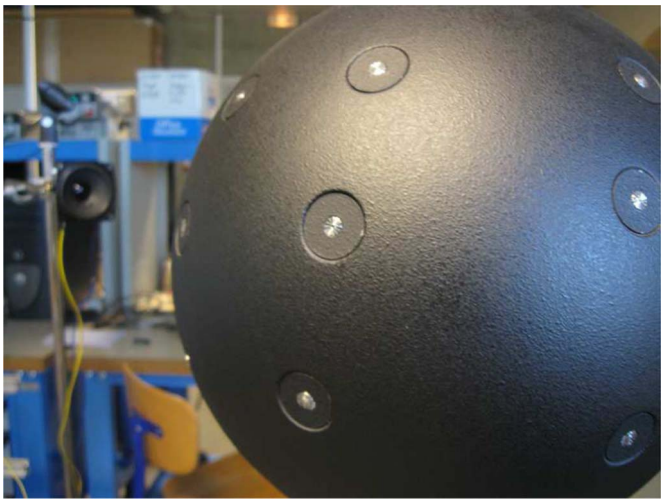

Fig. 6. Rigid sphere consisting of 36 microphones. The point-like source is represented by a small speaker placed at a distance 30 cm from the origin.

5. Real experiment

In this section, both methods are validated using the data measured by the rigid sphere of radius a=0.15 cm consisting of 36 microphones. Such an array is theoretically capable of operating up to the 5th order (of course, depending on the sampling scheme), however, because of a slight aliasing effect, the maximum order N=4 is assumed. Moreover, in the following example, the 4th order is significantly influenced by noise. A small speaker was used to represent a point-like source at a distance r_s = 0.3 m from the origin. The arrangement of the measurement is depicted in Fig. 6. In this experiment, the frequency f=400 Hz has been chosen to reduce slightly the value of kr_s = 2.22 in order better to satisfy the approximation condition when using a relatively low maximum order. For both methods, the determined distances are stated in Table 3. Again, the values in the gray-marked cells do not satisfy the approximation condition. It can also be seen that the result for the highest order is strongly influenced by noise, which transpires by the unfeasible distance 0.14 m in case of the approximation-based method and no intersection of the curves in case of no-approximation method. Therefore, in this case, only the determination based on the low orders using Eq. (10) is usable.

6. Discussion of uncertainty and Monte Carlo simulation

The precision of estimation of the source distance based on the proposed methods is influenced by several factors. The impact of these factors is discussed in this section, followed by their overall evaluation by the Monte Carlo simulation.

6.1. Discussion of uncertainty

As with any acoustic measurement, the measurements using a spherical microphone array suffer from the uncertainties of several quantities. The microphones qualitative properties (including the preamplifier), measurement front-end properties and environmental conditions (reflections, background noise) belong to the common sources of measurement uncertainties. Moreover, the accuracy of the sensor placement within the selected pattern of the phased array, and the sensors sensitivity and phase mismatch are specific sources of uncertainties using array-processing algorithms, including the proposed methods. Usually, it is possible to minimize the influence of mainly the specific sources of uncertainties using an array calibration – which in any case is necessary to perform before the arrays employment.

The overall uncertainty budget, including the quantity-estimation methods, their probability distributions and sensitivity weights, is very complex. For the purposes of this article, the use of a calibrated system (array and subsequent processing chain) is assumed, and the remaining quantities contributing to the overall measurement uncertainty are exhibited as random noise in the measured data. The influence of such noise in the data is evaluated using the Monte Carlo simulation.

Table 3
Real measured data. Determined values of r_s (m), the true value is r_s = 0.3 m and kr_s = 2.21.

Method	Order			
	0	1	2	3
Approx. r_s (m)	0.13	0.31	0.38	0.14
No approx. r_s (m)	0.31	0.35	0.30	–

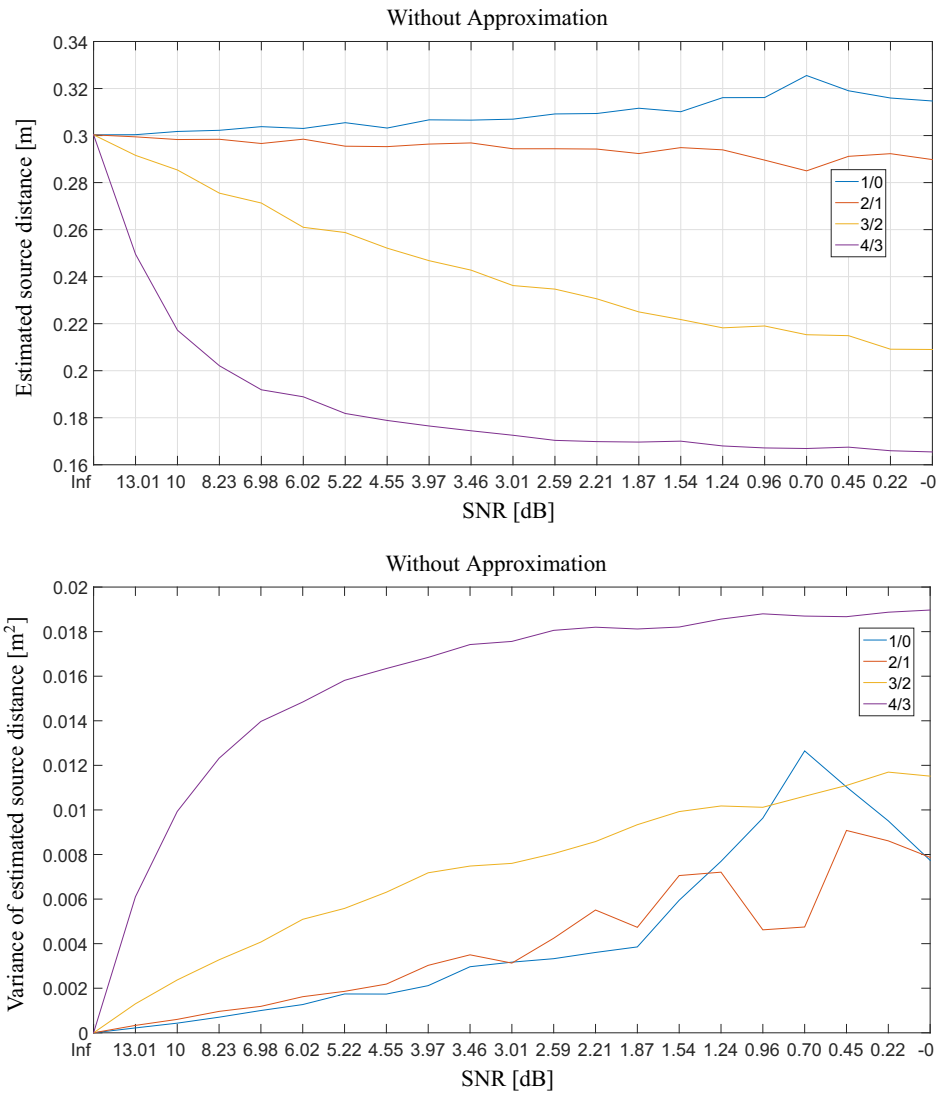

Fig. 7. Estimated source distance (top) together with its variance (bottom) using the method without the approximation for each mode ratio depending on the signal-to-noise ratio.

6.2. Monte Carlo simulation

The noise sensitivity of the proposed methods has been evaluated using the Monte Carlo simulation. The data (complex acoustics pressures) acquired using a rigid spherical array capable to operate up to 10th order of the spherical harmonics (same as one used for model validation in Section 4.1) have been modeled considering a point source located at a distance 30 cm from the array's origin. A zero-mean complex Gaussian noise with a variable variance has been iteratively added to the data, while the accuracy and variance of the source distance estimation have been evaluated by the proposed methods. Note that the noise is independent in both the time and space (between individual microphones). In the top part of Fig. 7, an estimated source distance using the method without the approximation is depicted for each mode ratio depending on the signal-to-noise ratio. In this case, the source frequency is equal to 200 Hz, which corresponds to the best distance estimation using a ratio of lower modes (1/0 or 2/1). Obviously, higher modes are not excited by the radiation of this source. In the bottom part of the same figure, the variance of the distance estimation is depicted in a similar way. In general, the method using approximation displayed worse performance and is not depicted here for brevity. In Fig. 8, the frequency dependence of the variance of the source distance estimation is shown for several signal-to-noise ratios for the method without approximation. The usability of a certain mode ratio for a given frequency band is clearly seen. Again, the method using approximation has shown worse performance. In general, increasing the number of microphones improves the overall performance of the methods.

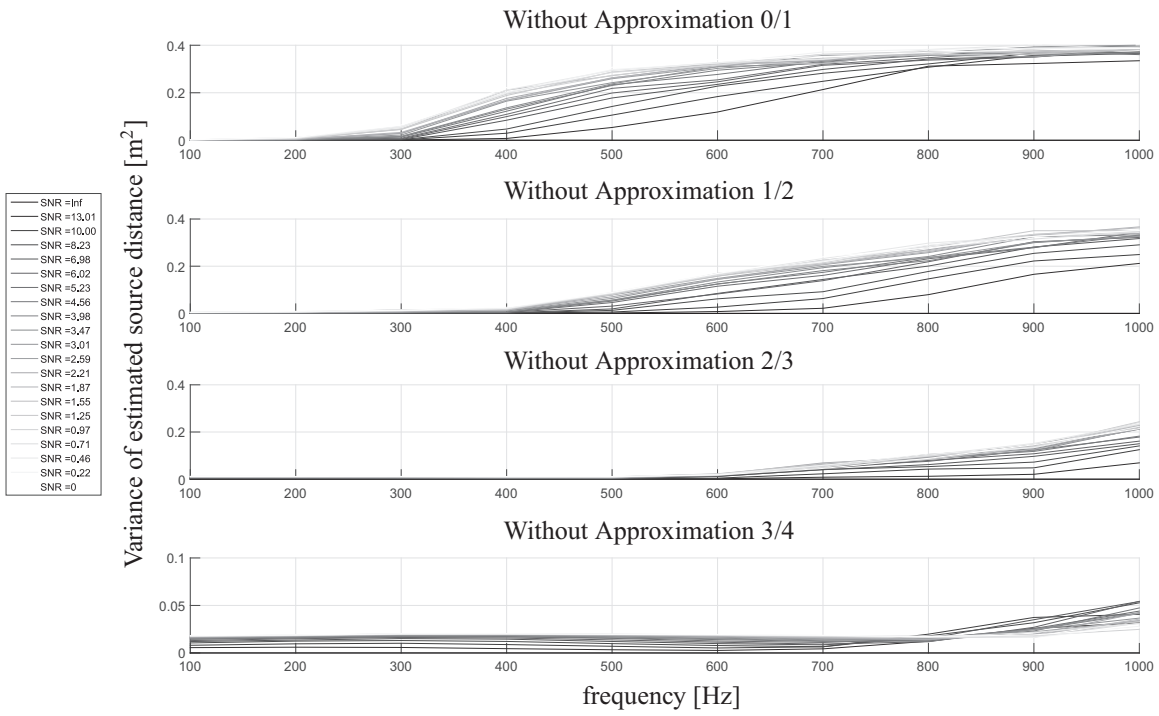

Fig. 8. Frequency dependence of the variance of the source distance estimation for several signal-to-noise ratios for the method without the approximation.

7. Conclusions

This paper focuses on the utilization of near-field information of data measured by the spherical microphone array in order to determine the distance to the origin of a spherical wave impinging on the array. The determination is based on the division of two adjacent overall spherical wave mode-strengths calculated using the Fourier coefficients of the spherical harmonics. Two methods, first using low-frequency approximation and the second using an original equation without approximation, are presented. The results of these methods as well as their comparison are presented with both model simulations (for different signal-to-noise ratios) and real measurement. The possibility of using low orders of spherical harmonics to determine the source distance has been shown. Concerning the design of an array while optimizing its near-field parameters, it is clear that both raising the maximum order and increasing the radius of the sphere will lead to the larger near-field extent.

The main advantages of the approximation-based method are its explicit formulation and therefore its ease of computation. However, regarding the opposite restrictions represented by the condition of approximation and the rapidly decaying behavior of the coefficients, it is always problematic to select the orders suitable for the source distance determination. On the other hand, the no-approximation method enables use of low orders, but the distance determination is more complicated and more computer-time-consuming. The robustness of the proposed method has been evaluated by sensitivity on noise using the Monte Carlo simulation. The method without the approximation has shown better performance over the method using the approximation. Moreover, increasing the number of microphones improves the overall performance.

This approach could find its application in situations in which the direct measurement of the distance to the source is impractical. Because of its functionality in the near-field, it could be connected with Near-field Acoustical Holography in order to determine the region of validity of the sound field reconstructions. The tracking of a point source moving in the near-field of an array, as well as the expansion of this approach to more complicated sources or multiple sources (e.g. by implementing sequential source separation/extraction methods), are the topics of the following research.

It should be noted that when the assumption of spherical wavefront is not fulfilled exactly, the method will not provide correct results. The accuracy of distance determination in the case of a disturbed spherical wavefront and its further influence to the PSS will be studied further.

Acknowledgment

This work was supported by CTU Project no. SGS13/193/OHK3/3T/13 Monitoring and modeling methods in acoustics.

References

[1] M. Park, B. Rafaely, Sound-field analysis by plane-wave decomposition using spherical microphone array, J. Acoust. Soc. Am. 118 (2005) 3094–3103.
[2] E.G. Williams, N. Valdivia, P.C. Herdic, Volumetric acoustic vector intensity imager, J. Acoust. Soc. Am. 120 (2006) 1887–1897.
[3] E.G. Williams, K. Takashima, Vector intensity reconstructions in a volume surrounding a rigid spherical microphone array, J. Acoust. Soc. Am. 127 (2010) 773–783.
[4] F. Jacobsen, G. Moreno-Pescador, E. Fernandez-Grande, J. rgen Hald, Near field acoustic holography with microphones on a rigid sphere, J. Acoust. Soc. Am. 129 (2011) 3461–3464.
[5] B. Rafaely, Plane-wave decomposition of the sound field on a sphere by spherical decomposition, J. Acoust. Soc. Am. 116 (2004) 2149–2157.
[6] B. Rafaely, Analysis and design of spherical microphone array, IEEE Trans. Speech Audio Process. 13 (2005) 135–143.
[7] E.G. Williams, Fourier Acoustic: Sound Radiation and Nearfield Acoustical Holography, Academic Press, London, 1999.
[8] B. Rafaely, Phase-mode versus delay-and-sum spherical microphone array processing, IEEE Signal Process. Lett. 12 (2005) 713–716.
[9] B. Rafaely, Methods for measuring acoustic radiation fields, J. Acoust. Soc. Am. 68 (1980) 404–411.
[10] E. Fisher, B. Rafaely, Near-field spherical microphone array processing with radial filtering, IEEE Trans. Audio, Speech Lang. Process. 19 (2011) 256–265.
[11] E. Fisher, B. Rafaely, The near-field spherical microphone array, in: Proceedings of the IEEE International Conference Acoustics, Speech, Signal Processing (ICASSP), 2008, pp. 5272–5275.
[12] H. Teutsch, Modal Array Signal Processing: Principles and Applications of Acoustic Wavefield Decomposition, Springer, Berlin, 2007.
[13] P. Castellini, M. Martarelli, Acoustic beamforming: analysis of uncertainty and meteorological performances, Mech. Syst. Signal Process. 22 (2008) 672–692.
[14] J.-H. Jeon, Y.-H. Kim, Localization of moving periodic impulsive source in a noisy environment, Mech. Syst. Signal Process. 22 (2008) 753–759.
[15] J. Meyer, G.W. Elko, Position independent close-talking microphone, Signal Process. 86 (2006) 1254–1259.
[16] S.F. Wu, N. Zhu, Blind extraction and localization of sound sources using point sources based approaches, J. Acoust. Soc. Am. 132 (2012) 904–917.
[17] A. Koutny, O. Jiricek, J.-H. Thomas, Holographic reconstruction of an incident field assuming the spherical waves scattered by a rigid sphere, in: Inter-noise Conference, 2013.